NANO LETTERS

2007
Vol. 7, No. 11
3547−3552

Increased Water Retention in Polymer Electrolyte Membranes at Elevated Temperatures Assisted by Capillary Condensation

Moon Jeong Park,[†,‡] Kenneth H. Downing,[§] Andrew Jackson,[||,£] Enrique D. Gomez,[†,‡] Andrew M. Minor,[#] David Cookson,[⊥] Adam Z. Weber,[+] and Nitash P. Balsara*[,†,‡,+]

Department of Chemical Engineering, Materials Sciences Division, Life Sciences Division, National Center for Electron Microscopy, Environmental Energy Technologies Division, Lawrence Berkeley National Laboratory, University of California, Berkeley, California 94720, NIST Center for Neutron Research, National Institute of Standards and Technology, Gaithersburg, Maryland 20899, Department of Materials Science and Engineering, University of Maryland, College Park, Maryland 20742, and Australian Synchrotron Research Program, Building 343, Advanced Photon Source, Argonne National Laboratory, 9700 South Cass Avenue, Argonne, Illinois 60439

Received October 10, 2007

ABSTRACT

We establish a new systematic methodology for controlling the water retention of polymer electrolyte membranes. Block copolymer membranes comprising hydrophilic phases with widths ranging from 2 to 5 nm become wetter as the temperature of the surrounding air is increased at constant relative humidity. The widths of the moist hydrophilic phases were measured by cryogenic electron microscopy experiments performed on humid membranes. Simple calculations suggest that capillary condensation is important at these length scales. The correlation between moisture content and proton conductivity of the membranes is demonstrated.

The fact that wet membranes dry up when heated in air appears to be an inescapable fact of life. The purpose of this paper is to describe the synthesis and characteristics of polymer electrolyte membranes (PEMs) comprising hydrophilic channels in a hydrophobic supporting structure that exhibit the opposite behavior, that is, their moisture content increases as the temperature of the surrounding air is increased at constant relative humidity (RH). This unusual behavior, which is seen when the width of the hydrophilic phases is less than 5 nm, leads to a significant enhancement in proton conductivity of the membranes at elevated temperatures. These membranes have the potential to increase the operating temperature of polymer electrolyte fuel cells (PEFCs).[1−7] Cells operating with H_2 and air as inputs and electric power and H_2O as the only outputs are of particular interest due to their ability to produce power without degrading the environment.

Current PEMs fall into two categories. The first category is based on copolymers wherein ion-containing hydrophilic groups are connected randomly to hydrophobic backbones. This category includes linear random fluorinated copolymers of polytetrafluroethylene and polysulfonyl fluoride vinyl ether, for example, perfluorosulfonic acid ionomer[1,2] (commercialized under the trademark Nafion), random linear and graft copolymers of polystyrene and poly(styrenesulfonic acid),[3,4] and sulfonated poly(ether ether ketone).[5,6] These systems have disordered morphologies in both dry and hydrated states due to the random location of the hydrophilic

* To whom correspondence should be addressed.
[†] Department of Chemical Engineering, University of California.
[‡] Materials Sciences Division, Lawrence Berkeley National Laboratory, University of California.
[§] Life Sciences Division, Lawrence Berkeley National Laboratory, University of California.
[#] National Center for Electron Microscopy, Lawrence Berkeley National Laboratory, University of California.
[+] Environmental Energy Technologies Division, Lawrence Berkeley National Laboratory, University of California.
[||] National Institute of Standards and Technology.
[£] University of Maryland.
[⊥] Argonne National Laboratory.

10.1021/nl072617l CCC: $37.00
Published on Web 10/26/2007

Table 1. Materials Used in Present Study

sample code[a]	molecular weight (PSS−PMB) (g/mol)	SL (%)	morphology in dry state	domain spacing (nm)	IEC (mmol/g)	water uptake at RH=98%, T = 25 °C (wt %)	water uptake at RH=98%, T = 90 °C (wt %)
P1 (0.877)	1.5−1.4K	17.8	disorder	4.67	0.877	26.2	25.2
P1 (1.513)	1.7−1.4K	30.7	disorder	4.80	1.513	62.8	66.4
P1 (1.582)	1.8−1.4K	32.1	gyroid	5.15	1.582	69.8	72.7
P1 (2.168)	2.0−1.4K	44.0	gyroid	5.16	2.168	81.6	91.0
P3 (0.950)	3.0−2.6K	18.9	LAM	7.28	0.950	27.1	30.4
P3 (1.005)	3.1−2.6K	20.9	LAM	7.53	1.005	33.2	40.3
P3 (1.608)	3.5−2.6K	31.9	HPL	8.08	1.608	58.4	65.7
P3 (2.226)	3.6−2.6K	44.3	HPL	8.28	2.226	77.1	85.0
P4 (0.845)	4.0−3.7K	17.4	LAM	9.05	0.845	29.1	34.7
P4 (1.073)	4.1−3.7K	22.1	gyroid	9.52	1.073	36.9	43.7
P4 (1.860)	4.6−3.7K	38.3	HPL	10.12	1.860	66.4	69.7
P4 (2.118)	4.8−3.7K	44.7	HPL	10.86	2.118	72.5	74.9
P5 (0.341)	5.1−4.6K	6.7	LAM	11.94	0.341	7.8	1.2
P5 (1.053)	5.6−4.6K	20.7	LAM+HPL	12.35+13.98	1.053	19.2	10.8
P5 (2.015)	6.4−4.6K	39.6	HPL	14.13	2.015	52.5	30.5
P5 (2.392)	6.9−4.6K	47	HEX	15.27	2.392	55.1	31.2
P5 (2.692)	7.1−4.6K	52.9	HEX	14.68	2.692	82.1	64.4
P9 (0.943)	10.6−8.7K	18.5	LAM+HPL	19.8+21.73	0.943	14.8	3.5
P9 (1.973)	12.1−8.7K	38.7	HEX	22.53	1.973	48.7	22.8
P9 (2.478)	12.8−8.7K	48.6	HEX	22.88	2.478	60.2	30.0
P9 (2.717)	13.2−8.7K	53.3	HEX	23.05	2.717	78.1	44.6
P48 (0.879)	52.8−55.0K	18.7	LAM+HPL	74.9+78.0	0.879	13.0	7.2
P48 (1.473)	55.0−55.0K	31.3	HEX	78.3	1.473	34.4	18.3
P48 (2.490)	61.0−55.0K	52.9	HEX	78.6	2.490	55.6	37.8
P48 (2.647)	61.6−55.0K	56.2	HEX	78.7	2.647	74.9	59.2

[a] Samples are labeled according to the nominal molecular weight of the nonsulfonated PS block and the IEC value. Sample P1 (1.582), for example, is the PSS−PMB block copolymer with a 1.4 kg/mol PS block with IEC = 1.582 mmol/g.

and hydrophobic moieties. PEMs in the second category are made from block copolymers with hydrophilic and hydrophobic blocks. Examples include sulfonated poly(styrene-b-isobutylene-b-styrene),[8] sulfonated poly(styrene-b-[ethylene-co-butylene]-b-styrene),[9] and sulfonated poly([vinylidene difluoride-co-hexafluoropropylene]-b-styrene).[10] In these materials, well-defined hydrophilic and hydrophobic domains are obtained in the dry state due to the balance of energetic and entropic driving forces.[11−13] Current PEFCs operate efficiently at low temperature (T < 80 °C) with ambient air but require RHs greater than 50%.[14−16] At elevated temperatures, water is lost from the PEMs due to system humidification constraints and material properties[17−19] resulting in a concomitant decrease in proton conductivity. The materials described below have the potential to overcome this limitation.

The present study is based on PEMs obtained from polystyrenesulfonate-*block*-polymethylbutylene (PSS-*b*-PMB) copolymers. Details concerning the synthesis and characterization procedures used are given in the Supporting Information. The characteristics of the polymers used in this study are summarized in Table 1. Nafion 117 serves as a benchmark for evaluating the efficacy of our membranes. Membranes were made by solvent casting PSS-*b*-PMB copolymers and drying the resulting films completely. The well-established phenomenon of microphase separation in block copolymers[11,12] leads to the spontaneous formation of hydrophilic PSS and hydrophobic PMB domains. The size of the hydrophilic phases depends mainly on the molecular weight of the PSS block while the extent of sulfonation controls the ion exchange capacity (IEC) of the membrane. Figure 1a plots the width of the dry hydrophilic phases as a function of molecular weight of the PSS block at IEC = 1.50 ± 0.12 mmol/g. The widths of the dry hydrophilic phases obtained in our membranes vary from 2.5 to 39.0 nm.

Proton conductivity of our membranes as a function of temperature was measured using AC impedance spectroscopy. Data were collected using a four-electrode probe (BekkTech conductivity clamp) over a frequency range of 1−10 000 kHz using a 1260 Solatron impedance analyzer.[20] Typical data are shown in Figure 1b where conductivity obtained from a series of PSS−PMB membranes at IEC = 2.25 ± 0.24 mmol/g and RH = 98% is plotted as a function of temperature. The samples were equilibrated under the specified conditions (T and RH) for 48 h before the measurement. It is evident that the temperature dependence of proton conductivity is not a smooth function of hydrophilic phase width (or equivalently PSS molecular weight). Instead we find that the data bunch up into 2 groups. Proton conductivity of membranes made from polymers P5, P9, and P48 (we refer to this as the high molecular weight group) decreases with increasing temperature when the 50 °C threshold is crossed. In contrast, proton conductivity obtained from membranes made from P1, P3, and P4 (we refer to this as the low molecular weight group) increases significantly with increasing temperature up to temperatures as high

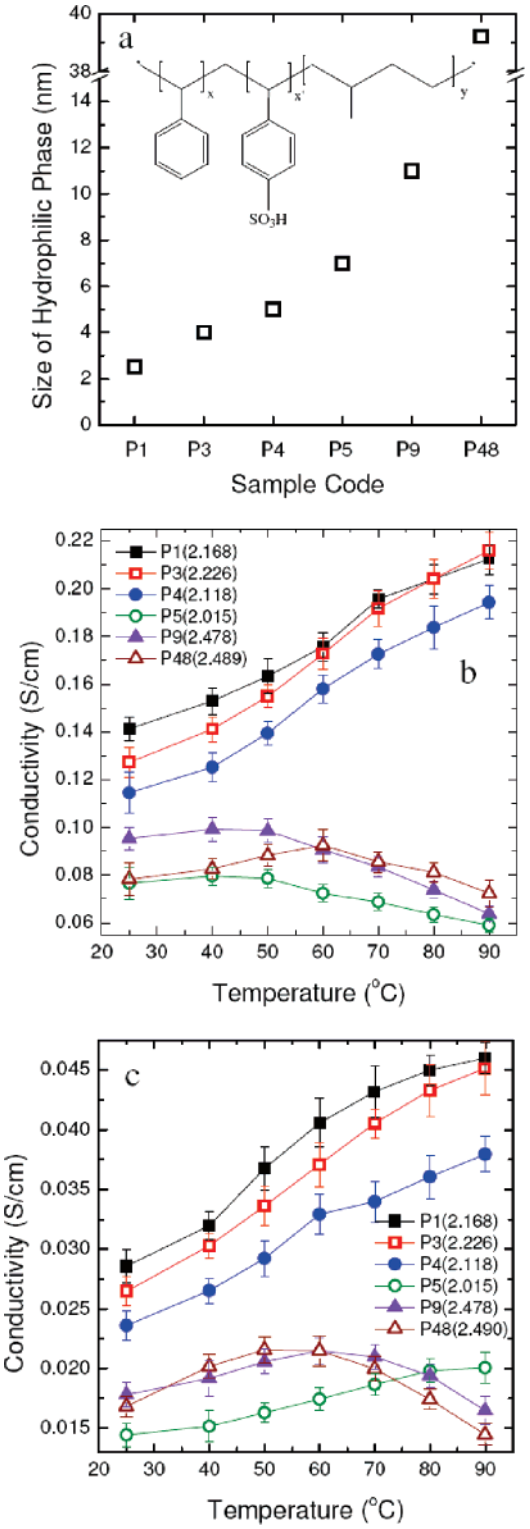

Figure 1. (a) Characteristic size of the hydrophilic phases of PSS-*b*-PMB series for a fixed IEC = 1.50 ± 0.12 mmol/g in the dry state. Proton conductivity results from PSS-*b*-PMBs as a function of temperature at fixed IEC values at (b) RH = 98% and (c) RH = 50%.

as 90 °C. In other words, there is a qualitative change in the proton conductivities of the membranes when the size of the hydrophilic phases is reduced from 6 to 5 nm.

For practical applications, the properties of membranes at low humidity are important. This is addressed in Figure 1c

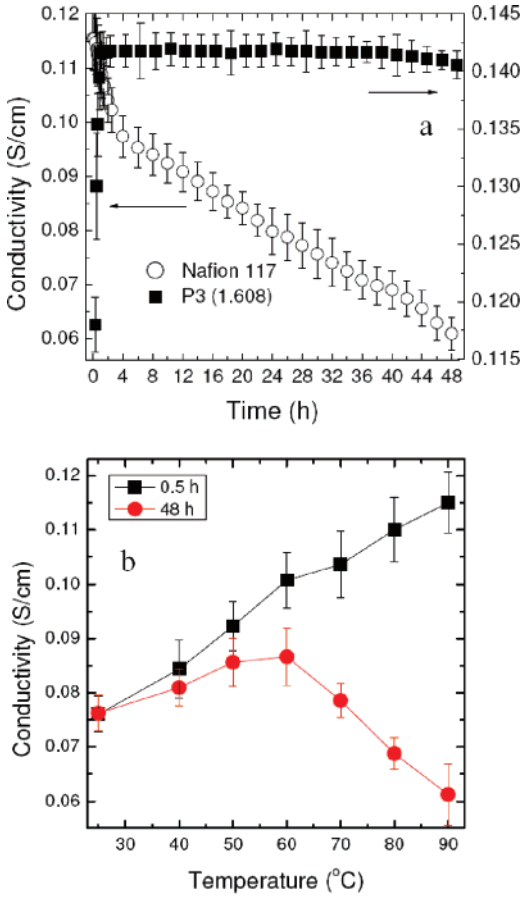

Figure 2. (a) Proton conductivity results from Nafion 117 and P3 (1.608) as a function of time at T = 90 °C and RH = 98%. (b) Proton conductivity results from Nafion 117 as a function of temperature at RH = 98% at two different equilibrium times.

where we report the temperature-dependent conductivity of our copolymer membranes with IEC = 2.25 ± 0.24 at RH = 50% (48 h equilibration time). We see a remarkable increase in conductivity with temperature up to 90 °C in the low molecular weight group. It is evident that the conductivity of our PEMs under dry conditions is significantly affected by the size of the hydrophilic phase. In particular, hydrophilic domains with a width of 2.5 nm exhibit the highest proton conductivity at 50% humidity.

Our decision to anneal our samples for 48 h at each temperature was the result of time-dependent studies on several samples. In Figure 2a, we show conductivity data obtained from a 180 μm thick P3 (1.608) membrane under RH = 98% after the sample temperature was switched from 25 to 90 °C. We found that proton conductivity reached a plateau after about 1 h. We thus believe that the conductivity (and other properties) measured after 48 h correspond to equilibrium behavior. In contrast, when the temperature of a 178 μm thick Nafion 117 membrane was switched from 25 to 90 °C, we found a rapid change for the first 4 h and then a steady decrease up to 48 h. In recent work, Newman and co-workers have demonstrated that the equilibration time of Nafion 117 can exceed 2.5 months.[21] The wide scatter of data obtained from Nafion membranes[1,10,22–26] is clearly due to this difficulty.

Figure 2b shows the temperature dependence of the proton conductivity data of Nafion 117 for annealing times of 0.5 and 48 h. The conductivity obtained with an annealing time of 0.5 h increases monotonically with increasing temperature, consistent with reports in refs 1, 2, and 24. In contrast, the conductivity obtained with an annealing time of 48 h is a nonmonotonic function of temperature, first increasing with increasing temperature up to 60 °C and then decreasing with increasing temperature. The long annealing time data in Figure 2b are consistent with data in refs 10, 25, and 26. We note in passing that the annealing protocol is not specified in many of the previous studies on Nafion. The long annealing time conductivity data obtained from Nafion 117 (Figure 2b) are similar to data obtained from the high molecular weight PSS−PMB samples (Figure 1b).

The temperature dependence of moisture content of our membranes at a fixed IEC value of 2.25 ± 0.24 is shown in Figure 3a (RH = 98%) and b (RH = 50%) with 48 h annealing time. Both λ_w, the number of water molecules retained per sulfonic acid group, and water uptake, the mass of water retained per unit mass of dry membrane, are shown in Figure 3. As was the case with the conductivity data, the ability of the membranes to retain water in PSS−PMB membranes is not a smooth function of hydrophilic phase width. Membranes made from the high molecular weight group dry up as they are heated above 70 °C. In contrast, the moisture content of the low molecular weight group increases with increasing temperature. While we have only shown data for one value of IEC, our conclusions regarding water retention hold at all of the IEC values, as summarized in Table 1, where membranes retain their structural integrity. To ensure that our conclusion about the temperature dependence of membrane moisture content is correct, we measured the water uptake by two independent methods and performed temperature-dependent in situ small angle neutron scattering experiments (in situ SANS) in a controlled D_2O/air environment, as described in the Supporting Information (Figure S1). It is evident that the significantly enhanced water retention seen in membranes made from the low molecular weight group leads to an increase in the overall proton transport rates (Figure 1b,c).

The dashed curve in Figure 3a represents the measured water uptake of Nafion 117 at RH = 98% with 48 h annealing time. The water uptake monotonically decreases upon increasing temperature in good agreement with previous experimental[21−23] and theoretical[27,28] studies.

Because the interactions between many polymers and solvents become more favorable with increasing temperature (the Flory−Huggins interaction parameter usually decreases with increasing temperature), solvent content of an open polymer membrane will increase with increasing temperature if evaporation is suppressed. We propose that this suppression occurs in our membranes due to capillary condensation. The confinement of fluids within narrow channels leads to a reduction in chemical potential due to curvature-related (that is, meniscus) effects. A measure of the decrease in chemical potential is the decrease of the vapor pressure of the confined fluid. Using the Kelvin and Young−Laplace equations,[29] the

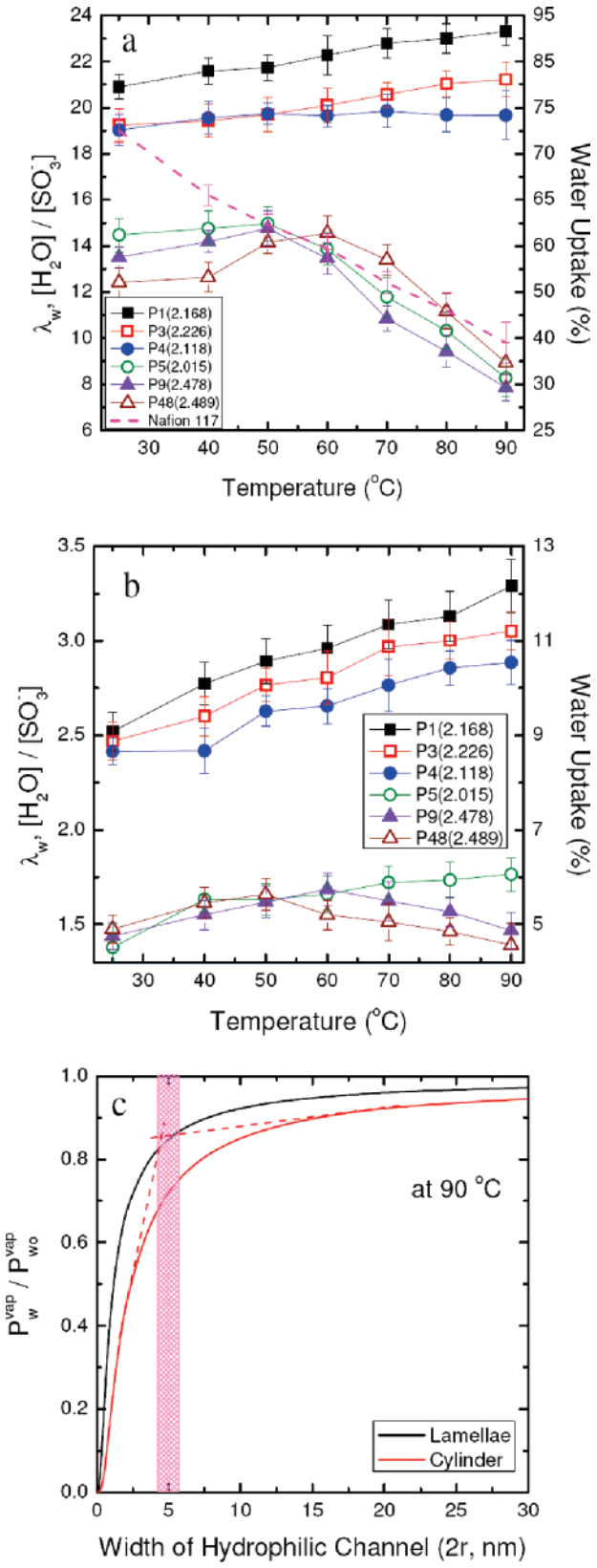

Figure 3. Water uptake results from PSS-*b*-PMBs as a function of temperature at fixed IEC values at (a) RH = 98% and (b) RH = 50%. λ_w is the number of water molecules per sulfonic acid group and % water uptake = (mass of water in membrane/mass of dry membrane) × 100. The right-hand ordinate in (a) does not apply to the Nafion data. (c) Dependence of the vapor pressure of water on the width of the confining hydrophilic channel (eq 1).

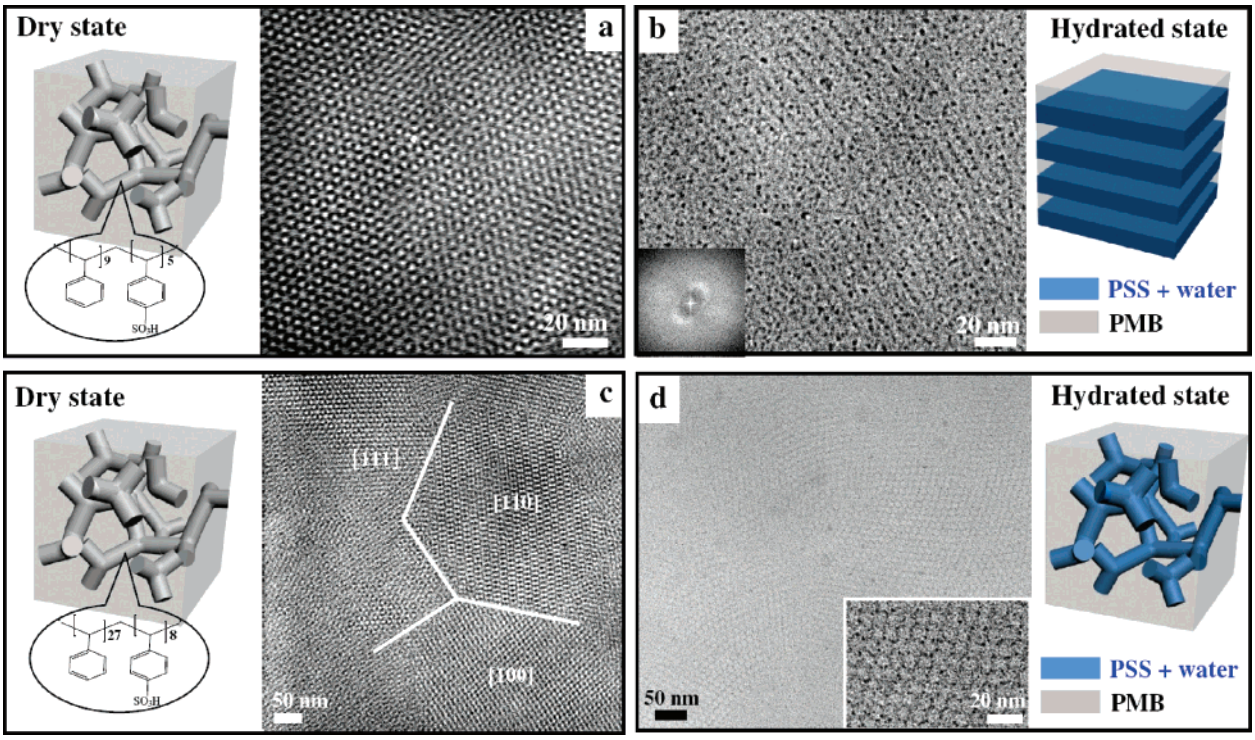

Figure 4. (a) Cross-sectional TEM image of stained P1 (1.582) in dry state. (b) Cryo-TEM image and fast Fourier transform inset of hydrated sample for unstained P1 (1.582). (c) TEM image of stained P4 (1.073) in dry state with gyroid morphology showing three different grain orientations having 4-fold [100], 3-fold [111], and 2-fold [110] symmetry. (d) Cryo-TEM image of unstained hydrated P4 (1.073) sample showing the (111) plane. The inset box in (d) shows the image obtained with higher magnification. For dry samples, PSS domains appear dark due to RuO_4 staining. The images of hydrated samples are obtained without staining and thus, the dark regions in (b) and (d) represent the water-rich domains. Schematics depict the change in channel geometry as a result of hydration.

vapor pressure of water contained within a channel, p_w^{vap}, is given by

$$p_w^{vap} = p_{w,o}^{vap} \exp\left(-\frac{2aV_w\gamma \cos\theta}{wRT}\right) \quad (1)$$

where $p_{w,o}^{vap}$ is the normal vapor pressure of water, γ is the surface tension of water, R is the ideal-gas constant, T is the absolute temperature, V_w is the molar volume of water, θ is the contact angle between water and the pore surface, w is the width of the pore (diameter of cylindrical pores and width of lamellar pores), and constant a depends on channel geometry (1 and 2 for lamellae and cylinders, respectively). Solving the above temperature-implicit equation for ambient pressure and assuming perfect wetting ($\theta = 0$) leads to results shown in Figure 3c. A rapid decrease of the pressure within hydrophilic channels is seen when w approaches 5 nm. Note that the hydrophilic channels in our membranes are not isolated water channels but comprise coexisting water and PSS molecules. Further studies are needed to determine if the water molecules in these channels are homogeneously distributed throughout the phase. Improved theories that account for capillary condensation effects in the presence of a PSS brush are needed for a more quantitative comparison between theory and experiment.

Determining the hydrated morphologies of our PEMs is essential for establishing the underpinnings of our water retention measurements. This has proven to be challenging because typical sample environments used in experiments that probe the molecular scale morphology of polymers such as electron microscopy and X-ray and neutron scattering do not allow for controlled humidity experiments. In the case of Nafion and random copolymer-based PEMs, for example, it is clear that dispersed hydrophilic domains in the dry state coalesce to give continuous water-filled channels in the hydrated state,[10−12] but the exact geometry of the channels remains to be established. This is due in part to the polydispersity of the channels. Surprisingly, the same difficulty seems to apply to block copolymer-based PEMs. For reasons that are unclear, all previous studies on hydrated block copolymers have concluded that the order becomes poorer upon hydration.[8−10,30] There is thus a lack of basic understanding of the relationship between hydrated morphology and proton conductivity in PEMs.

In Figure 4a we show a traditional transmission electron microscopy (TEM) image obtained on sample P1(1.582) in the dry state indicating the presence of a gyroid morphology (see Figure 2S in Supporting Information for detailed analysis with small-angle X-ray scattering).[31] To determine the hydrated morphology, thin sections with nominal thicknesses between 50 and 100 nm obtained using a cryo-microtome were immersed in water, and hydrated sections were frozen using liquid N_2 and transferred to a JEOL-3100-FEF electron microscope equipped with an Omega energy filter and cryo-transfer stage. Experimental details (energy filtering, defocus levels, dose rates for preserving the hydrated polymer

structures, and contrast enhancement) are given in Supporting Information. In Figure 4b, we show a cryo-TEM image of an 80 nm thick specimen of hydrated P1(1.582), where the presence of a lamellar phase with 2.5 nm wide hydrophilic phases are seen. It is important to note that the TEM image in Figure 4b is obtained without staining. Because the electron density of the hydrophilic domains (PSS + water) is higher than that of the hydrophobic domains (PMB), the dark regions in Figure 4b represent the water-rich domains. To our knowledge, the image in Figure 4b represents the first electron micrograph of undoped hydrated channels in any PEM. All previous studies[3,8−10] have obtained images of the hydrated channels doped with heavy ions. This can introduce artifacts due to effects such as distortion of soft nanostructures by heavy metals, interfacial segregation of the metals, etc. The speckles in the images may be due to imaging artifacts or amorphous features of the water-filled channels. In situ SANS studies confirm the humidity-induced morphological transition described above (see Figure 3S in Supporting Information). In some cases, the morphology obtained in the dry and hydrated states is identical. This is demonstrated in Figure 4c,d where we show TEM results of dry and wet versions of P4 (1.073). Bicontinuous gyroid phases with 9.5 nm domain spacing are obtained in both cases. The length scale of the honeycomb-like structure from hydrated P4 (1.073) (Figure 4d) matches the periodicity along the [111] projection in the dry state (Figure 4c). Contrary to current literature,[8−10,30] our studies indicate that while the addition of water can affect the geometry of the channels, there is no loss of order upon hydration.

In summary, we have created microstructured membranes, composed of hydrophilic and hydrophobic domains that are more effective at extracting water from the surrounding air when the temperature of the air is increased at constant relative humidity up to temperatures as high as 90 °C. This unexpected behavior is seen when the width of the hydrophilic domains is less than 5 nm. Not surprisingly, the proton conductivity of these membranes also increases with increasing temperature. While this property may enable the construction of more efficient, high-temperature polymer electrolyte fuel cells, our main accomplishment is that we have uncovered a new methodology for systematically controlling the moisture content of microstructured materials. Becausee water is an important component of many synthetic and biological systems, our membranes may be useful for other applications such as protective clothing for dry environments.

Acknowledgment. We gratefully acknowledge the Director, Office of Science, Office of Basic Energy Sciences (BES), of the US Department of Energy (DOE) under Contract No. DE-AC02-05CH11231 for major support, the use of TEM facilities of LBNL Life Sciences Division, the use of SAXS instruments at the Advanced Photon Source (APS) supported by BES, DOE, under Contract No. DE-AC02-06CH11357, the National Science Foundation (NSF)/DOE under Grant CHE-0535644, and the use of SANS facilities at NIST supported by the NSF under Agreement No. DMR-0504122.

Supporting Information Available: Polymer synthesis and characterization, water uptake measurements, in situ SANS, temperature-dependent in situ SANS of hydrated samples, SAXS, and TEM. This material is available free of charge via the Internet at http://pubs.acs.org.

References

(1) Hickner, M. A.; Ghassemi, H.; Kim, Y. S.; Einsla, B. R.; McGrath, J. E. *Chem. Rev.* **2004**, *104*, 4587−4611.
(2) Mauritz, K. A.; Moore, R. B. *Chem. Rev.* **2004**, *104*, 4535−4585.
(3) Ding, J. F.; Chuy, C.; Holdcroft, S. *Chem. Mater.* **2001**, *13*, 2231−2233.
(4) Ding, J. F.; Chuy, C.; Holdcroft, S. *Adv. Funct. Mater.* **2002**, *12*, 389−394.
(5) Kopitzke, R. W.; Linkous, C. A.; Anderson, H. R.; Nelson, G. L. *J. Electrochem. Soc.* **2000**, *147*, 1677−1681.
(6) Rikukawa, M.; Sanui, K. *Prog. Polym. Sci.* **2000**, *25*, 1463−1502.
(7) Kreuer, K. D. In *Handbook of Fuel Cell − Fundamentals, Technology and Applications*; Vielstich, W., Lamm, A., Gasteiger, H. A. Eds; John Wiley & Sons Ltd: Chichester, UK, 2003; Vol. 3, Part 3.
(8) Elabd, Y. A.; Napadensky, E.; Walker, C. W.; Winey, K. I. *Macromolecules* **2006**, *39*, 399−407.
(9) Kim, J.; Kim, B.; Jung, B. *J. Membrane. Sci.* **2002**, *207*, 129−137.
(10) Shi, Z. Q.; Holdcroft, S. *Macromolecules* **2005**, *38*, 4193−4201.
(11) Leibler, L. *Macromolecules* **1980**, *13*, 1602−1617.
(12) Khandpur, A. K.; Förster, S.; Bates, F. S.; Hamley, I. W.; Ryan, A. J.; Bras, W.; Almdal, K.; Mortensen, K. *Macromolecules* **1995**, *28*, 8796−8806.
(13) Cho, B.-K.; Jain, A.; Gruner, S. M.; Wiesner, U. *Science* **2004**, *305*, 1598−1601.
(14) Anantaraman, A. V.; Gardner, C. L. *J. Electroanal. Chem.* **1996**, *414*, 115−120.
(15) Choi, P.; Jalani, N. H.; Datta, R. *J. Electrochem. Soc.* **2005**, *152*, E123−E130.
(16) Shao, Y.; Yin, G.; Wang, Z.; Gao, Y. *J. Power Sources* **2007**, *167*, 235−242.
(17) Kreuer, K. D.; Paddison, S. J.; Spohr, E.; Schuster, M. *Chem. Rev.* **2004**, *104*, 4637−4678.
(18) Jiang, R. C.; Kunz, H. R.; Fenton, J. M. *J. Power Sources* **2005**, *150*, 120−128.
(19) Gebel, G. *Polymer* **2000**, *41*, 5829−5838.
(20) Cahan, B. D.; Wainright, J. S. *J. Electrochem. Soc.* **1993**, *140*, L185−L189.
(21) Onishi, L. M.; Prausnitz, J. M.; Newman, J. *J. Phys. Chem. B* **2007**, *111*, 10166−10173.
(22) Hinatsu, J. T.; Mizuhata, M.; Takenaka, H. *J. Electrochem. Soc.* **1994**, *141*, 1493−1498.
(23) Broka, K.; Ekdunge, P. *J Appl. Electrochem.* **1997**, *27*, 117−123.
(24) Maréchal, M.; Souquet, J.-L.; Guindet, J.; Sanchez, J.-Y. *Electrochem. Commun.* **2007**, *9*, 1023−1028.
(25) Slade, S.; Campbell, S. A.; Ralph, T. R.; Walsh, F. C. *J. Electrochem. Soc.* **2002**, *149*, A1556−A1564.
(26) Lee, C. H.; Park, H. B.; Lee, Y. M.; Lee, R. D. *Ind. Eng. Chem. Res.* **2005**, *44*, 7617−7626.
(27) Fukerko, P.; Hsinga, I.-M. *J. Electrochem. Soc.* **1999**, *146*, 2049−2053.
(28) Ge, S.; Li, X.; Yi, B.; Hsinga, I.-M. *J. Electrochem. Soc.* **2005**, *152*, A1149−A1157.
(29) Dullien, F. A. L. *Transp. Porous Media* **1991**, *6*, 581−606.
(30) Won, J.; Park, H. H.; Kim. Y. J.; Choi, S. W.; Ha, H. Y.; Oh, I.-H.; Kim, H. S.; Kang, Y. S.; Jin, K. J. *Macromolecules* **2003**, *36*, 3228−3234.
(31) Benedicto, A. D.; OBrien, D. F. *Macromolecules* **1997**, *30*, 3395−3402.

NL072617L